

JAERI-Research

96-062



SOLUTION FOR A WINDOW COATING PROBLEM DEVELOPED  
IN THE JT-60U THOMSON SCATTERING SYSTEM

November 1996

Hidetoshi YOSHIDA, Osamu NAITO,  
Takaki HATAE and Akira NAGASHIMA

日本原子力研究所  
Japan Atomic Energy Research Institute

本レポートは、日本原子力研究所が不定期に公刊している研究報告書です。

入手の問合わせは、日本原子力研究所研究情報部研究情報課（〒319-11 茨城県那珂郡東海村）あて、お申し越してください。なお、このほかに財団法人原子力弘済会資料センター（〒319-11 茨城県那珂郡東海村日本原子力研究所内）で複写による実費頒布をおこなっております。

This report is issued irregularly.

Inquiries about availability of the reports should be addressed to Research Information Division, Department of Intellectual Resources, Japan Atomic Energy Research Institute, Tokai-mura, Naka-gun, Ibaraki-ken, 319-11, Japan.

© Japan Atomic Energy Research Institute, 1996

編集兼発行 日本原子力研究所  
印 刷 いばらき印刷(株)

Solution for a Window Coating Problem Developed  
in the JT-60U Thomson Scattering System

Hidetoshi YOSHIDA, Osamu NAITO, Takaki HATAE and Akira NAGASHIMA

Department of Fusion Plasma Research  
Naka Fusion Research Establishment  
Japan Atomic Energy Research Institute  
Naka-machi, Naka-gun, Ibaraki-ken

(Received October 22, 1996)

For an exact measurement of fusion plasmas with higher electron temperature, the following two methods which can solve a window coating problem were developed in the JT-60U Thomson scattering system. One is an *in situ* monitoring method which can infer a window transmission with sufficient precision from a known attenuation of the deposited film. The other is an *in situ* window cleaning method which removes the film on the basis of a laser blow-off technique. As the results of the extensive investigations, the existence of chromatic upper limit has been found in the recovered transmission after the laser blow-off cleaning, however, which gives systematic errors only of less than 3% to the apparent measurement for both electron density and temperature at 10 keV or less. The attenuation itself was unchanged before and after the laser blow-off cleaning. So the first method can be also applicable to the window after the laser blow-off cleaning. A complementary use of both the methods against the window coating problem can be expected to provide the Thomson scattering measurement of high T<sub>e</sub> plasmas with durable reliability and sufficient precision in the present tokamaks and also the ITER.

Keywords: Window Coating Problem, JT-60U, Thomson Scattering, Polyacrylonitrile,  
Window Transmission, Attenuation, Laser Blow-off, ITER

J T-60 U トムソン散乱測定装置における観測窓コーティング問題の解決策

日本原子力研究所那珂研究所炉心プラズマ研究部

吉田 英俊・内藤 磨・波多江仰紀

長島 章

(1996年10月22日受理)

高電子温度の核融合プラズマを正確に測定することを目的として、J T-60 U トムソン散乱測定装置において観測窓の汚れ問題を解決する2つの方法を開発した。第1番目の方法は、蒸着膜の減衰係数を既知として観測窓を真空容器に取付けた状態でその光透過率を実用上十分な精度で推定する方法である。第2番目の方法は、同じく観測窓を真空容器に取付けた状態でレーザーブローオフ技術に基づいて蒸着膜を観測窓から除去する方法である。広範かつ系統的な調査の結果、レーザーブローオフ法による透過率回復には上限があることが判明したが、それでも10keV以下の高温プラズマに対して、除去後の測定における系統誤差は電子温度及び密度ともに3%以下まで軽減できることを明らかにした。またレーザーブローオフ前後で蒸着膜の減衰係数自身には変化が無いことから、第1番目の方法との併用が可能であることも明らかにした。現存及びITER等将来のトカマク装置でのトムソン散乱測定装置による高温プラズマ測定において、両方法の相補的な活用により観測窓の汚れ問題に対して長期的な測定信頼性と十分な測定精度を確保することができるものと期待される。

## Contents

1. Introduction .....	1
2. Characteristics of Deposited Films .....	2
2.1 Window Transmission .....	2
2.2 Film Composition .....	3
2.3 Film Thickness .....	4
3. <i>In Situ</i> Monitoring Method for Coated Window Transmission .....	5
4. Laser Blow-off Based <i>In Situ</i> Window Cleaning .....	7
4.1 Testing Arrangement .....	7
4.2 Transmission Recovery .....	8
4.3 Area Recovery .....	9
5. Discussions .....	9
6. Conclusion .....	11
Acknowledgments .....	12
References .....	13

## 目 次

1. 序 論 .....	1
2. 蒸着膜の特徴 .....	2
2.1 観測窓の透過率 .....	2
2.2 蒸着膜の組成 .....	3
2.3 蒸着膜の膜厚 .....	4
3. コーティングされた観測窓透過率のその場監視方法 .....	5
4. レーザブローオフ法によるその場観測窓洗浄方法 .....	7
4.1 試験方法 .....	7
4.2 透過率の回復 .....	8
4.3 面積の回復 .....	9
5. 議 論 .....	9
7. 結 論 .....	11
謝 辞 .....	12
参考文献 .....	13

## 1. Introduction

The degradation of a viewing window transmission is still one of practical problems to be solved on visible plasma diagnostics. Through many plasma discharges thin films colored dark brown are gradually deposited on the inner surface of the window, which attenuates the light from plasmas to be measured and also gives rise to the spectrum distortion due to the chromatic dependence of its transmission property. Especially in Thomson scattering diagnostics, the coated window causes a systematic underestimation not only for electron density  $n_e$  but for electron temperature  $T_e$ . This problem is emphasized more in the measurement with a large scattering angle and also for high  $T_e$  plasma, because in such cases the Thomson scattering spectrum stretches toward shorter wavelength region, where the coated window transmission decreases more.<sup>1), 2)</sup> With the progress of tokamak experiments, high electron temperature exceeding around 10 keV has been demonstrated in large fusion devices such as JT-60U,<sup>3)</sup> TFTR<sup>4)</sup> and JET.<sup>5)</sup> On the other hand, the frequent vacuum break needed for the replacement of the coated window with a fresh one has become hard, owing to the operational necessity of keeping the first wall clean and the limited access to the activated vessel components. To cope with such a problem without a vacuum break of the vessel, several kinds of coating protection and transmission correction techniques have been developed as follows: (i) mechanical shutters installed in front of the inner window surface, (ii) replaceable protective cover glasses stacked with a window shutter,<sup>6)</sup> (iii) *in situ* spectral calibration using a white plate provided by a special probe taken in and out the vessel<sup>7)</sup> and (iv) *in situ* window transmission monitoring by comparing the plasma light transmitted through the coated window and the laser *blown-off* window.<sup>8)</sup> The second approach can periodically keep the window clean and lasts it longer than the first one. The third and fourth approaches are effective against a temporal change of the window transmission.

On the other hand, also *in situ* window cleaning methods have been developed. A *localized* electron cyclotron resonance discharge with pure hydrogen was investigated at the initial stage.<sup>9)</sup> This window cleaning method, however, necessitates the special configuration that produces the resonance magnetic field *locally*, close to the coated window. Recently a laser blow-off based window cleaning has been recognized as the useful method that can provide the transmission recovery *in situ*. The first demonstration based on this method was performed *in atmosphere* by Narihara et al.<sup>10)</sup> for the JIPP TII-U Thomson scattering window. They used a Nd:YAG laser with laser energy per pulse of ~0.4 J, pulse width of ~30 ns and repetition rate of 30 Hz. Also in the JET LIDAR Thomson scattering system, the effectiveness of this method has been demonstrated by Brown et al.<sup>11)</sup> with the low energy density fixed at 0.25 J/cm<sup>2</sup> using a 3 J, 0.3 ns and 0.5 Hz ruby laser.<sup>12)</sup> The excellence of the JET Thomson

scattering is that they have adopted the laser blow-off *in situ* cleaning method in combination with the window transmission monitoring method mentioned above for solving the window coating problem. This combined method, however, requires the special configuration such as a backscattering geometry.

The main purpose of this paper is to propose a novel approach to the *in situ* window transmission monitoring based on an idea of using a known attenuation of the deposited film, and also to present the latest results of the laser blow-off window cleaning that can give us sufficient grounds for its practical effectiveness. In Section 2 the fundamental features of deposited films on their growth, composition and thickness are revealed for the first time using the coated windows used in the JT-60/JT-60U Thomson scattering system for the last eight years. The expression that can infer the coated window transmission is derived in Section 3, using a known chromatic attenuation of the film and Rayleigh scattering or bremsstrahlung light. The basic properties of laser blow-off based window cleaning for the transmission recovery and the area recovery are investigated in connection with the laser energy per unit area and the irradiation number of successive laser pulses in Section 4. Finally the efficiency of laser blow-off cleaning and the comparison of attenuation before and after laser blow-off are discussed in Section 5. The conclusion in this work is summarized in Section 6.

## 2. Characteristics of Deposited Films

### 2.1. Window Transmission

Figure 1 illustrates the collection optics in the JT-60U Thomson scattering system, the two viewing windows made of synthetic silica at *INIA* port for measuring the edge plasma and at *RI* port for the core plasma, and the corresponding mechanical shutters. Working gas was hydrogen for JT-60 from 1986 to 1989, and mainly deuterium for JT-60U after 1991. The vacuum vessel has been almost kept at about 300°C during each experimental period. Inconel 625 has been a main material of the vacuum vessel. From 1986 to 1989 the Thomson scattering measurement was made only through the *INIA* port using a mechanical shutter without a remote control function. The transmission of the thin-film-deposited windows is shown in Fig. 2. The periods of each window attached to the vacuum vessel are presented in Table I with the typical plasma configurations, operational records and the first wall materials of JT-60/JT-60U. The window coating problem had been enhanced since the first wall tiles made of titanium carbide (TiC) coated molybdenum (Mo) was replaced by those made of graphite in 1988. From Fig. 2 and Table I it is understood that the window

scattering is that they have adopted the laser blow-off *in situ* cleaning method in combination with the window transmission monitoring method mentioned above for solving the window coating problem. This combined method, however, requires the special configuration such as a backscattering geometry.

The main purpose of this paper is to propose a novel approach to the *in situ* window transmission monitoring based on an idea of using a known attenuation of the deposited film, and also to present the latest results of the laser blow-off window cleaning that can give us sufficient grounds for its practical effectiveness. In Section 2 the fundamental features of deposited films on their growth, composition and thickness are revealed for the first time using the coated windows used in the JT-60/JT-60U Thomson scattering system for the last eight years. The expression that can infer the coated window transmission is derived in Section 3, using a known chromatic attenuation of the film and Rayleigh scattering or bremsstrahlung light. The basic properties of laser blow-off based window cleaning for the transmission recovery and the area recovery are investigated in connection with the laser energy per unit area and the irradiation number of successive laser pulses in Section 4. Finally the efficiency of laser blow-off cleaning and the comparison of attenuation before and after laser blow-off are discussed in Section 5. The conclusion in this work is summarized in Section 6.

## 2. Characteristics of Deposited Films

### 2.1. Window Transmission

Figure 1 illustrates the collection optics in the JT-60U Thomson scattering system, the two viewing windows made of synthetic silica at *INIA* port for measuring the edge plasma and at *RI* port for the core plasma, and the corresponding mechanical shutters. Working gas was hydrogen for JT-60 from 1986 to 1989, and mainly deuterium for JT-60U after 1991. The vacuum vessel has been almost kept at about 300°C during each experimental period. Inconel 625 has been a main material of the vacuum vessel. From 1986 to 1989 the Thomson scattering measurement was made only through the *INIA* port using a mechanical shutter without a remote control function. The transmission of the thin-film-deposited windows is shown in Fig. 2. The periods of each window attached to the vacuum vessel are presented in Table I with the typical plasma configurations, operational records and the first wall materials of JT-60/JT-60U. The window coating problem had been enhanced since the first wall tiles made of titanium carbide (TiC) coated molybdenum (Mo) was replaced by those made of graphite in 1988. From Fig. 2 and Table I it is understood that the window



transmission decreases from the original value of 94% with the number of plasma discharges as well as the exposure time to discharge cleaning of Taylor type (TDC), irrespective of the number of disruptions. Since 1991 the remote-controlled mechanical shutters installed at *INIA* and *RI* ports have worked so that it is closed except for during plasma discharges. As a result, the severe deterioration of window transmission has been possibly avoided as shown in Fig. 2, exclusive of the transmission with a shutter trouble occurred in the first half of 1992.

Although  $T_e$  did not exceed largely above 5 keV for most of the plasma discharges at the periods of 1987 to 1989,<sup>13)</sup> the systematic errors of underestimation at  $T_e$  of 5 keV would reach at most to 3%, 6%, 11% and 18% for  $T_e$  and to directly 16%, 30%, 49% and 50% for  $n_e$  for the corresponding windows of sample No. 1, 2, 3 and 4. Taking advantage of small scattering angle ( $54^\circ\sim 72^\circ$ ) and low  $T_e$  plasmas, it was possible to correct the electron density by a comparison between the line density integrated along the vertical beam line and the FIR interferometer data. Such a correction can not be always applicable to higher  $T_e$  measurement especially with a large scattering angle, however, because the correction factor is not uniform spatially; the extent of the spectral modulation and also the resultant underestimation differs largely among the spatial points ranging from low  $T_e$  region to high  $T_e$  one and from small scattering angle to large one.

## 2.2. Film Composition

The color of the deposited films varies from light brown to dark one with decrease in the transmission. Graphite is generally thought to be a major component of the coated film. The film coated with pure carbon is brown, too.<sup>14)</sup> However, the following fact suggests that the films may include other components but pure carbon: the chromatic attenuation of the films has not been always the same in detail for each experimental period as shown in Fig. 2.

In order to look at light element contents, the qualitative analysis based on an electron spectroscopy for chemical analysis (ESCA) method was carried out for the film deposited on the window sample of No. 2. The film was peeled off from the window surface by a standard carbon tape with an adhesive agent made from carbon (C), oxygen (O) and hydrogen (H). The three different samples were prepared for the analysis: I) the peeled-off film attached to the carbon tape through the adhesive agent mentioned above, II) the standard carbon tape with the adhesive agent alone and III) the Ar<sup>+</sup>-etching-suffered sample of I). The role of Ar<sup>+</sup> bombardment through a glow discharge is to remove the contents of the adhesive agent. From the sample I) the detected elements were C, O, nitrogen (N) and silicon (Si), while N was not found completely in the ESCA spectrum from the sample II). Figure 3

shows the wide scanning spectrum of the sample I) and III) plotted against a binding energy, indicating that C is thought to be the major component of the film together with a small amount of N.<sup>1)</sup> Because O and Si observed in the sample I) were extremely reduced after Ar<sup>+</sup> etching, they seem to be residual elements that come from the window material (SiO<sub>2</sub>). Especially for oxygen, there might be the possibility that it is included in the film as H<sub>2</sub>O or hydroxide, too. It should be noted that H can not be detected in principle by ESCA. However, it seems to be a natural guess that the coated film would include H, since the detected elements of C and N are thought to be polymerized possibly together with H through the normal hydrogen discharges. The detailed analysis of the C<sub>1s</sub> spectral shape showed a resemblance to that of *polyacrylonitrile* (polymer of CH<sub>2</sub>CHCN) with -C=C bond rather than -C≡C bond. Namely the whole spectrum of the narrow scanning ESCA for C<sub>1s</sub> was separated into four spectra with different peak positions and relative intensities based on the corresponding chemical bond such as -CH<sub>2</sub>, -C=N, -C≡N and C-C conjugate or -C=O bond. Each separated spectrum shape was compared with that of *polyacrylonitrile*. As a result, it was found that each peak position and relative intensity of the four separated spectra was almost consistent with that of *polyacrylonitrile* with -C=N bond rather than -C≡N bond. *Polyacrylonitrile* with -C=C bond, which can be easily changed by heat from that with -C≡C bond, is also brown.<sup>15)</sup> Then a resin based on a polymer such as *polyacrylonitrile* can be considered to be one of strong possibilities as a chemical structure of the deposited film.

Next to check up on heavy element contents, the quantitative analysis using inductively coupled plasma-atomic emission spectroscopy (ICP-AES) was made for the film of the window sample of No. 3. As a result, the following heavy elements with very small quantities were detected from the effective window area of 220 mm diameter: Fe (16 μg), Ni (8 μg) and Cr (2 μg) which are the vessel-related materials of Inconel 625 and SUS 304, and Zn (15 μg), Al (10 μg), V (8 μg), Ti (2 μg) and Mn (less than 1 μg). It is unknown at present what kind of state these heavy elements exist in the deposited films: for example, as the original materials alone, as the chemisorbed ones or as the metallic oxide or the pure elements with layer structure. As one of possible explanations for the slight change of the chromatic attenuation for every experimental period, however, it may be brought about by the deposits of these heavy elements, while most of the attenuation must be determined by the resin composed of light elements such as C, H and N.

### 2.3. Film Thickness

A thickness of deposited film was measured by a spectroscopic ellipsometer. The thickness and the complex refractive index of the film can be generally determined through a non-linear

least squares fit of the three-phase optical model (air as an ambient medium, a film and  $\text{SiO}_2$  as an substrate) and the two measured ellipsometric parameters for the wavelength range of 300 nm to 800 nm. The errors in this measurement is expected to be less than 10% for the film thickness more than 5 nm.<sup>16)</sup> The measured thickness of the films  $d$  for the window samples of No. 10, 12 and 17 is plotted against the fractional window transmission  $T/T_0$  in Fig. 4, where  $T_0$  is the original window transmission of 94%. The measured film thickness of the sample window of No. 12, which suffered not only the normal plasma discharges but the cleaning discharges (TDC) for several hours, exceeds 100 nm at  $T/T_0=0.3\sim 0.4$  in the wavelength of 500 nm. In the same wavelength, on the meanwhile, the thickness of the evaporated pure carbon film was estimated at roughly 50 nm or less with a chromatic transmission similar to the sample window No. 12.<sup>14)</sup> This discrepancy makes it clear that the film composition differs from pure carbon only, supporting the previous result in Subsection 2.2. From the above measurement it was found that the film is distributed with slightly different thickness on the whole window surface; the thickness measured near the fringe region is about 20% thicker than that at the center region in the *INIA* window, and 30% in the *RI* one.

### 3. *In Situ* Monitoring Method for Coated Window Transmission

A transmission of coated window with a chromatic dependence can be expressed generally as

$$T(\lambda) = T_0 \exp[-\alpha(\lambda)t], \quad (1)$$

where  $\alpha(\lambda)$  is a wavelength-dependent attenuation of the coated film, and  $t$  the film thickness that is considered to be independent of wavelength. Using the self-consistent measured data on the transmission  $T(\lambda)$  and the corresponding film thickness  $d$  investigated in Subsection 2.3, the attenuation  $\alpha(\lambda)$  can be estimated as

$$\alpha(\lambda) = (1/d) \ln[T_0/T(\lambda)]. \quad (2)$$

Figure 5 shows the obtained attenuation plotted as a function of wavelength. It should be noted that there is a little difference in the chromatic attenuation of the *INIA* window (sample No. 10) and the *RI* window (sample No. 12 and 17). This slight discrepancy seems to be based on the difference of the metallic ingredients between them mentioned in Subsection 2.2, which originates in the difference of the two ports in location. So for pursuing higher accuracy, therefore, a polynomial regression to obtain the empirical expression of the attenuation

least squares fit of the three-phase optical model (air as an ambient medium, a film and  $\text{SiO}_2$  as an substrate) and the two measured ellipsometric parameters for the wavelength range of 300 nm to 800 nm. The errors in this measurement is expected to be less than 10% for the film thickness more than 5 nm.<sup>16)</sup> The measured thickness of the films  $d$  for the window samples of No. 10, 12 and 17 is plotted against the fractional window transmission  $T/T_0$  in Fig. 4, where  $T_0$  is the original window transmission of 94%. The measured film thickness of the sample window of No. 12, which suffered not only the normal plasma discharges but the cleaning discharges (TDC) for several hours, exceeds 100 nm at  $T/T_0=0.3\sim 0.4$  in the wavelength of 500 nm. In the same wavelength, on the meanwhile, the thickness of the evaporated pure carbon film was estimated at roughly 50 nm or less with a chromatic transmission similar to the sample window No. 12.<sup>14)</sup> This discrepancy makes it clear that the film composition differs from pure carbon only, supporting the previous result in Subsection 2.2. From the above measurement it was found that the film is distributed with slightly different thickness on the whole window surface; the thickness measured near the fringe region is about 20% thicker than that at the center region in the *INIA* window, and 30% in the *RI* one.

### 3. *In Situ* Monitoring Method for Coated Window Transmission

A transmission of coated window with a chromatic dependence can be expressed generally as

$$T(\lambda) = T_0 \exp[-\alpha(\lambda)t], \quad (1)$$

where  $\alpha(\lambda)$  is a wavelength-dependent attenuation of the coated film, and  $t$  the film thickness that is considered to be independent of wavelength. Using the self-consistent measured data on the transmission  $T(\lambda)$  and the corresponding film thickness  $d$  investigated in Subsection 2.3, the attenuation  $\alpha(\lambda)$  can be estimated as

$$\alpha(\lambda) = (1/d) \ln[T_0/T(\lambda)]. \quad (2)$$

Figure 5 shows the obtained attenuation plotted as a function of wavelength. It should be noted that there is a little difference in the chromatic attenuation of the *INIA* window (sample No. 10) and the *RI* window (sample No. 12 and 17). This slight discrepancy seems to be based on the difference of the metallic ingredients between them mentioned in Subsection 2.2, which originates in the difference of the two ports in location. So for pursuing higher accuracy, therefore, a polynomial regression to obtain the empirical expression of the attenuation

had better be separately made for the *INIA* film and for the *RI* film. The following results were obtained for the expression of the film attenuation of the *INIA* window as

$$\alpha_{\text{INIA}}(\lambda) = 0.0645 - 1.71 \times 10^{-4} \lambda + 1.20 \times 10^{-7} \lambda^2, \quad (3)$$

and for that of the *RI* window as

$$\alpha_{\text{RI}}(\lambda) = 0.0439 - 9.92 \times 10^{-5} \lambda + 6.23 \times 10^{-8} \lambda^2, \quad (4)$$

with an error of less than 7% and an applicable wavelength range of 400 nm to 700 nm. However, even if the polynomial regression is made for the combined data of the *INIA* and *RI* films, the degradation of accuracy is nothing but less than 13% with using the following expression as

$$\alpha_{\text{INIA \& RI}}(\lambda) = 0.0483 - 1.15 \times 10^{-4} \lambda + 7.50 \times 10^{-8} \lambda^2. \quad (5)$$

Such a wide applicability of the obtained expression of attenuation would be based on the unchangeableness of the major composition of the deposited films. The film composition itself seems to depend mainly on the first wall materials. So the chromatic window transmission can be inferred widely, if only the film thickness is measured with the window mounted to the vessel.

The following illumination sources are useful for estimating the above thickness *in situ*: Rayleigh scattering light ( $\lambda=694.3$  nm for a ruby laser) from occasional calibrations and bremsstrahlung light (for example,  $\lambda=523.0$  nm stably available for the practical use with bandpass filters in commercial base) from reference plasma discharges produced frequently. The Rayleigh scattering light is preferable to the latter in terms of stable reproducibility as an illumination source and high S/N ratio of the detector system using other equipments of the existing Thomson scattering system. On the other hand, the bremsstrahlung light to the former in terms of availability for the frequent measurement of window transmission daily or weekly. The following procedure of measuring the film thickness is based on the use of the Rayleigh scattering light. A Rayleigh scattering light intensity  $N_0$  is obtained through a fresh window, while  $N_R$  through the coated one. If all components of the system are kept in the same condition as at the first Rayleigh scattering calibration after the window replacement, the ratio  $N_0/N_R$  gives an information on the deposited film thickness  $t_R$  as follows:

$$t_R = (1/\alpha_R) \ln(T_0/T_R) = (1/\alpha_R) \ln(N_0/N_R), \quad (6)$$

where  $T_R=T(\lambda_R)$ ,  $\alpha_R=\alpha(\lambda_R)$  and  $\lambda_R=694.3$  nm for a ruby laser. Inserting  $t_R$  in Eq. (1) and using

the known attenuation  $\alpha(\lambda)$  as in Eqs. (3) and (4), we can obtain the expression for the chromatic window transmission as

$$T(\lambda) = T_0 \exp[-\alpha(\lambda)t_R]. \quad (7)$$

It should be noted that  $t_R$  and the resultant  $T(\lambda)$  can be estimated individually for each spatial point through this method, which is advantageous to a non-uniformity of the deposited film distribution on the window surface mentioned in Subsection 2.3.

Supposing the errors generated through the measurement of the empirical film attenuation and the Rayleigh scattering light are 7% and 5%, respectively, the systematic error of the inferred transmission is expected to be about 1% at the wavelength of 700nm and less than 2% even at 500 nm for a slightly coated window with a film thickness of 10 nm. Even for a severely coated window with film thickness of 50 nm, its transmission can be inferred within an error of 5% at 700 nm and less than 9% even at 500 nm. Assuming that  $t_R$  is accurately estimated as  $t_R = (1/\alpha_R) \ln(T_0/T_R)$ , the above inferring expression is possible to reproduce the chromatic transmission within an error of 10% even at 500 nm for the windows which have been coated through the JT-60U discharges during the experimental periods for the last five years. In this case the calculated  $t_R$  does not exceed largely 70 nm. Using the *in situ* inferring method of this type, the temporal change of the coated window transmission can be monitored occasionally in accordance with Rayleigh-scattering-based calibration. Naturally the frequently updated  $t_R$  can give more precise correction for the coated window transmission. So if the stable bremsstrahlung light with good reproducibility in the limited wavelength is used instead, the estimation of the film thickness could be performed more frequently.

## 4. Laser Blow-off Based *In Situ* Window Cleaning

### 4.1. Testing Arrangement

A laser blow-off based cleaning test was performed using the windows of sample No. 8 and 9 (*INIA*), and 12, 14, 16 and 17 (*RI*) in Table I. They were removed from the JT-60U vessel and mounted again on another small vessel with a pumping system as illustrated in Fig. 6. A Nd:YAG laser, which capabilities are 2.0~2.2 J laser energy per pulse, 10 ns pulse width, 25 mm beam diameter and 10 Hz repetition rate, was used for irradiating the coated window. The beam diameter on the window surface of the film side was varied from 7 mm to 40 mm, avoiding the window damages. The corresponding laser energy per unit area, or the laser energy density  $\epsilon$ , ranged from 0.16 to 5.3 J/cm<sup>2</sup>, which is defined as  $\epsilon \equiv E_{laser}/S_{beam}$ .

the known attenuation  $\alpha(\lambda)$  as in Eqs. (3) and (4), we can obtain the expression for the chromatic window transmission as

$$T(\lambda) = T_0 \exp[-\alpha(\lambda)t_R]. \quad (7)$$

It should be noted that  $t_R$  and the resultant  $T(\lambda)$  can be estimated individually for each spatial point through this method, which is advantageous to a non-uniformity of the deposited film distribution on the window surface mentioned in Subsection 2.3.

Supposing the errors generated through the measurement of the empirical film attenuation and the Rayleigh scattering light are 7% and 5%, respectively, the systematic error of the inferred transmission is expected to be about 1% at the wavelength of 700nm and less than 2% even at 500 nm for a slightly coated window with a film thickness of 10 nm. Even for a severely coated window with film thickness of 50 nm, its transmission can be inferred within an error of 5% at 700 nm and less than 9% even at 500 nm. Assuming that  $t_R$  is accurately estimated as  $t_R = (1/\alpha_R) \ln(T_0/T_R)$ , the above inferring expression is possible to reproduce the chromatic transmission within an error of 10% even at 500 nm for the windows which have been coated through the JT-60U discharges during the experimental periods for the last five years. In this case the calculated  $t_R$  does not exceed largely 70 nm. Using the *in situ* inferring method of this type, the temporal change of the coated window transmission can be monitored occasionally in accordance with Rayleigh-scattering-based calibration. Naturally the frequently updated  $t_R$  can give more precise correction for the coated window transmission. So if the stable bremsstrahlung light with good reproducibility in the limited wavelength is used instead, the estimation of the film thickness could be performed more frequently.

## 4. Laser Blow-off Based *In Situ* Window Cleaning

### 4.1. Testing Arrangement

A laser blow-off based cleaning test was performed using the windows of sample No. 8 and 9 (*INIA*), and 12, 14, 16 and 17 (*RI*) in Table I. They were removed from the JT-60U vessel and mounted again on another small vessel with a pumping system as illustrated in Fig. 6. A Nd:YAG laser, which capabilities are 2.0~2.2 J laser energy per pulse, 10 ns pulse width, 25 mm beam diameter and 10 Hz repetition rate, was used for irradiating the coated window. The beam diameter on the window surface of the film side was varied from 7 mm to 40 mm, avoiding the window damages. The corresponding laser energy per unit area, or the laser energy density  $\epsilon$ , ranged from 0.16 to 5.3 J/cm<sup>2</sup>, which is defined as  $\epsilon \equiv E_{laser}/S_{beam}$ .

Here  $E_{laser}$  is the laser energy per pulse and  $S_{beam}$  the *beam-hit* area on the coated film. A focal point was set at the back of the mounted window, otherwise *in atmosphere* most of the laser energy would be lost before reaching to the window through such a gas breakdown produced near there by extremely high electric field of the laser. The pumping system was capable of providing a vacuum of up to the order of  $10^{-3}$  Pa.

## 4.2. Transmission Recovery

The transmission recovery of coated windows was investigated in terms of its dependence on the laser energy density and also the number of successive laser pulses. The coated window of sample No. 16 was used for this purpose. Figure 7 shows the nonlinear dependence of the transmission recovery on  $\epsilon$  observed at 500 nm with a single Nd: YAG laser pulse. The deposited film is removed well with increase in  $\epsilon$ . Especially for  $\epsilon \geq 2$  J/cm<sup>2</sup>, the regained transmission reached its maximum of 86% at 400 nm, 89% at 500 nm as shown in Fig. 7, 93% at 600 nm and perfectly 94%, the same as the original transmission, at 700 nm and over, and seemed to be saturated for larger  $\epsilon$ . This result agrees with the previous work<sup>10</sup> on the energy density needed for an almost complete blow-off by a single laser pulse, but differs in the existence of a wavelength-dependent upper limit for the regained transmission. It is interesting to note that even at lower  $\epsilon$  of 0.20 J/cm<sup>2</sup> the blow-off effect was observed.

Figure 8 shows the regained transmission at 500 nm plotted against the irradiation number of successive laser pulses. For the blow-off operation with  $\epsilon = 0.92$  J/cm<sup>2</sup>, about twenty successive Nd: YAG laser pulses were required for obtaining the maximum of the regained transmission. For further reference of the blow-off performance with higher energy density ( $\sim 2$  J/cm<sup>2</sup>) and different wavelength, the JT-60U ruby laser was also used<sup>17)</sup>. As shown in this figure, the same capability as the Nd: YAG laser was obtained. There also existed the wavelength-dependent upper limit for the transmission recovery. The maximum of the regained transmission for each wavelength was almost the same as that obtained through a single Nd: YAG laser pulse with  $\epsilon \geq 2$  J/cm<sup>2</sup>. This upper limit for the transmission recovery was investigated more in terms of the different film thickness and the blow-off operation *in vacuum* or *in atmosphere* using the windows of sample No. 8 and 14 in addition to No. 16. As a result, almost the same wavelength-dependent upper limit was observed as shown in Fig. 9, irrespective of the film thickness and the operation *in atmosphere* or *in vacuum*. The maximum of the transmission recovering rate  $\gamma$ , defined as the ratio of the recovered transmission to the original one, was 0.91 to 0.94 at 400 nm, 0.95 at 500 nm, 0.98 to 1.00 at 600 nm and  $\sim 1.00$  at 700 nm and more. Nevertheless with the above upper limit after laser blow-off



cleaning, the systematic error of underestimation can be reduced to less than 2.5% and 3.0% for  $T_e$  and  $n_e$  estimation, respectively, for the high  $T_e$  plasma measurement of  $T_e \leq 10$  keV as shown in Fig. 10.

### 4.3. Area Recovery

The energy density dependence of the area recovering rate  $\eta$  is shown in Fig. 11 for a single pulse operation of the Nd: YAG laser, where  $\eta$  is defined as the ratio of  $S_{blow-off}$  the *blown-off* area with  $\gamma > 0.95$ , to  $S_{beam}$ . For the blow-off operation with  $\epsilon > 3$  J/cm<sup>2</sup>, the *blown-off* area was distributed over the whole *beam-hit* area. The area recovering rate also depends on the irradiation number of successive laser pulses as shown in Fig. 12. As to the blow-off operation with  $\epsilon \geq 0.33$  J/cm<sup>2</sup>, almost the complete area recovery was attained within 500 successive irradiation of laser pulses. A series of photographs is shown in Fig. 13 for the *blown-off* area of the sample window No.12 irradiated by successive Nd: YAG laser pulses with  $\epsilon = 0.33$  J/cm<sup>2</sup>. These photographs are identical with the data plotted in Fig. 12 with the same irradiation numbers as indicated figures and the same laser energy per unit area as 0.33 J/cm<sup>2</sup>. The *blown-off* area increased with the irradiation number of laser pulses and spread all over the *beam-hit* area after 500 successive pulses, while the residual interference fringes was observed clearly within 100 successive irradiation of laser pulses. The blow-off operation with very low  $\epsilon$  takes extremely long time; the operation with  $\epsilon$  of 0.16 J/cm<sup>2</sup> takes 60 times longer time to achieve the area recovering rate of  $\sim 0.9$  compared with that of 0.33 J/cm<sup>2</sup>. This is related with the fact that the interference modulation are hard to be removed in the case with very low  $\epsilon$ .

## 5. Discussions

As a measure of the efficiency to sweep quickly the deposited film off the whole window, the sweeping speed defined as

$$Sp = S_{blow-off} / (N_L / f) = f E_{laser} \eta / (\epsilon N_L) \quad (8)$$

is introduced,<sup>10)</sup> where  $N_L$  the irradiation number of successive laser pulses required for removing the deposited film almost perfectly,  $f$  the repetition rate of laser. Figure 14 shows the dependence of  $Sp$  and  $N_L$  on the energy density of the Nd: YAG laser. Here the plotted data satisfy the condition that both of the transmission recovering rate and the area recovering rate exceed 0.95. The highest sweeping speed was about 12 cm<sup>2</sup>/s obtained at 1.8 J/cm<sup>2</sup> in a

cleaning, the systematic error of underestimation can be reduced to less than 2.5% and 3.0% for  $T_e$  and  $n_e$  estimation, respectively, for the high  $T_e$  plasma measurement of  $T_e \leq 10$  keV as shown in Fig. 10.

### 4.3. Area Recovery

The energy density dependence of the area recovering rate  $\eta$  is shown in Fig. 11 for a single pulse operation of the Nd: YAG laser, where  $\eta$  is defined as the ratio of  $S_{blow-off}$  the *blown-off* area with  $\gamma > 0.95$ , to  $S_{beam}$ . For the blow-off operation with  $\epsilon > 3$  J/cm<sup>2</sup>, the *blown-off* area was distributed over the whole *beam-hit* area. The area recovering rate also depends on the irradiation number of successive laser pulses as shown in Fig. 12. As to the blow-off operation with  $\epsilon \geq 0.33$  J/cm<sup>2</sup>, almost the complete area recovery was attained within 500 successive irradiation of laser pulses. A series of photographs is shown in Fig. 13 for the *blown-off* area of the sample window No.12 irradiated by successive Nd: YAG laser pulses with  $\epsilon = 0.33$  J/cm<sup>2</sup>. These photographs are identical with the data plotted in Fig. 12 with the same irradiation numbers as indicated figures and the same laser energy per unit area as 0.33 J/cm<sup>2</sup>. The *blown-off* area increased with the irradiation number of laser pulses and spread all over the *beam-hit* area after 500 successive pulses, while the residual interference fringes was observed clearly within 100 successive irradiation of laser pulses. The blow-off operation with very low  $\epsilon$  takes extremely long time; the operation with  $\epsilon$  of 0.16 J/cm<sup>2</sup> takes 60 times longer time to achieve the area recovering rate of  $\sim 0.9$  compared with that of 0.33 J/cm<sup>2</sup>. This is related with the fact that the interference modulation are hard to be removed in the case with very low  $\epsilon$ .

## 5. Discussions

As a measure of the efficiency to sweep quickly the deposited film off the whole window, the sweeping speed defined as

$$Sp = S_{blow-off} / (N_L / f) = f E_{laser} \eta / (\epsilon N_L) \quad (8)$$

is introduced,<sup>10)</sup> where  $N_L$  the irradiation number of successive laser pulses required for removing the deposited film almost perfectly,  $f$  the repetition rate of laser. Figure 14 shows the dependence of  $Sp$  and  $N_L$  on the energy density of the Nd: YAG laser. Here the plotted data satisfy the condition that both of the transmission recovering rate and the area recovering rate exceed 0.95. The highest sweeping speed was about 12 cm<sup>2</sup>/s obtained at 1.8 J/cm<sup>2</sup> in a

single pulse operation. Comparing the results shown in Figs. 8 and 12, it is understood that  $N_L$  is determined by the requirement for the area recovery rather than for the transmission recovery. It is important to note that the maximum of the sweeping speed is attained at the high energy density of around  $2 \text{ J/cm}^2$  with  $N_L=1$  in this work and also in the previous work<sup>10)</sup> using Nd: YAG lasers. This means that the Nd: YAG laser operation with higher  $\varepsilon$  and smaller  $N_L$  is more effectual in blow-off window cleaning than that with lower  $\varepsilon$  and larger  $N_L$ . In such an effective case, the blow-off operation can be performed without worry about the problem of the residual interference modulation discussed in Subsection 4.3.

In order to infer the window transmission over an extended period of time, it is worth while examining a change in the attenuation before and after the blow-off cleaning. Figure 15 shows the above comparisons: (a) for the *RI* window of sample No. 17 coated only through the normal plasma discharges, and (b) for the *INIA* window of sample No. 9 slightly coated through the normal plasma discharges and also strongly stained by foreign matters such as melted Viton. Then the attenuation of No.9 window differed from the empirical expression given as Eq. (4) in the chromatic dependence. The film thickness was reduced by the laser blow-off from 21 nm to only around 2 nm for the normally coated window of No. 17, and from 54 nm to 13 nm for the stained window of No. 9. We can say from Fig. 15 that the difference in the attenuation before and after the blow-off cleaning is so small to infer the *blown-off* window transmission precisely, and that the change in the film composition may be also small.

As a future plan in the JT-60U Thomson scattering system and also other visible diagnostics, the combination of laser blow-off based *in situ* window cleaning method with *in situ* window transmission inferring method is very attractive. Using the window transmission inferred by this method, the correction of apparently measured  $T_e$  and  $n_e$  can be made in the data processing. Frequent renewal of the film thickness can give more precise correction, which may be possibly made by short and frequent measurements of Rayleigh scattering light intensity or by routine measurements of bremsstrahlung light intensity from the reference discharges. If the measured film thickness exceeds the limit over which the accuracy of the inferring method deteriorates, the laser blow-off based *in situ* window cleaning can be implemented for the complete transmission recovery without vacuum break of the vessel. As to the *in situ* window cleaning tools, a portable type Nd: YAG laser with higher energy and higher repetition rate, and also a computer-controlled laser scan system or a multi-joint light guide system are desirable, which are now available in commercial base.

## 6. Conclusion

The window coating problem has been one of the remaining issues to be solved for long years in visible plasma diagnostics. For establishing the exact measurement of  $T_e$  and  $n_e$  profiles even in higher  $T_e$  plasmas, the following results were obtained in this work using the coated windows of the JT-60/JT-60U Thomson scattering system spanning ten years.

- (1) The main composition of the film deposited on the inside of the viewing window surface during normal plasma discharges could be guessed to be a resin such as *polyacrylonitrile* with a small amount of metals from the qualitative and quantitative analyses. This result motivated us to develop the following two methods for solving a window coating problem in Thomson scattering system.
- (2) As the first approach, the *in situ* monitoring method of the window transmission was successfully demonstrated with sufficient precision of less than 10% for the first time in the JT-60U Thomson scattering system. This method can infer a window transmission from a known attenuation of the deposited film and its thickness estimated by the ratio of Rayleigh scattering intensities with and without the film. It is a distinct feature that this method does not necessitate a special layout like a LIDAR Thomson scattering system nor an additional apparatus other than an existing Thomson scattering system.
- (3) As the second approach, the *in situ* window cleaning method based on a laser blow-off technique was extensively investigated. As a result, the existence of the chromatic upper limit was found in the recovered transmission after the laser blow-off cleaning. However, it was also confirmed that this upper limit gives systematic errors only of less than 3% to the apparent measurement for both  $n_e$  and  $T_e$  at 10 keV or less. The maximum sweeping speed, which is a measure of the efficiency to remove quickly the film, has reached up to 12 cm<sup>2</sup>/s with  $\epsilon$  of 1.8 J/cm<sup>2</sup> in a single pulse operation, indicating that the laser operation with higher  $\epsilon$  is more effectual in blow-off window cleaning.
- (4) The attenuation itself is unchanged before and after the laser blow-off cleaning. So the *in situ* monitoring method of the window transmission is also usefully applicable to the window after the laser blow-off cleaning. A complementary use of both the methods can be expected to provide the Thomson scattering measurement of high  $T_e$  plasmas with durable reliability and sufficient precision in the present tokamaks and also the ITER.

## **Acknowledgments**

The authors would like to appreciate Dr. T. Matoba and Dr. D. Johnson (Plasma Physics Laboratory of Princeton University) for useful discussions and suggestions, and Dr. M. Mori and Dr. H. Kishimoto for their continuous support and encouragement. The authors gratefully acknowledge Y. Suzuki and D. Kazama for their technical assistance in operating the Nd:YAG laser and measuring the window transmission and thickness.

## References

- <sup>1</sup>Y. Miura, H. Yoshida, T. Sakuma, O. Yamashita, A. Nagashima and T. Matoba, JAERI-M 90-167, "Effect of Coated Window on Electron Temperature and Density Evaluation in JT-60 Thomson scattering Diagnostic" (1990).
- <sup>2</sup>D. H. McNeill, *Rev. Sci. Instrum.* **61**, 1263 (1990).
- <sup>3</sup>H. Yoshida and the JT-60 Team, *Fusion Technology* **26**, 406 (1994).
- <sup>4</sup>D. W. Johnson, V. Arunasalam, C. W. Barnes, S. H. Batha, G. Bateman, M. Beer, M. G. Bell, R. Bell, M. Bitter, N. L. Bretz, R. Budny, C. E. Bush, S. Cauffman, C. S. Chang, Z. Chang, D. S. Darrow, R. Dendy, W. Dorland, H. H. Duong, R. Durst, P. C. Efthimion, D. Ernst, H. Evenson, N. Fisch, R. Fisher, R. J. Fonck, E. Fredrickson, G. Y. Fu, T. Fujita, H. P. Furth, N. Gorelenkov, B. Grek, L. R. Grisham, G. Hammett, R. J. Hawryluk, W. Heidbrink, H. W. Herrmann, K. W. Hill, J. Hosea, H. Hsuan, M. Hughes, A. Janos, D. L. Jassby, F. C. Jobs, L. C. Johson, J. Kamperschroer, J. Kesner, M. Kotschenreuther, H. Kugel, P. H. LaMarche, B. LeBlanc, F. M. Levinton, J. Machuzak, R. Majeski, D. K. Mansfield, E. S. Marmor, E. Mazzucato, M. Mael, J. McChesney, K. M. McGuire, G. McKee, D. M. Meade, S. S. Medley, D. R. Mikkelsen, S. V. Mirnor, D. Mueller, R. Nazikian, M. Osakabe, D. K. Owens, H. Park, W. Park, P. Parks, S. F. Paul, M. Petrov, C. K. Phillips, M. Phillips, A. L. Qualls, A. Ramsey, M. H. Redi, G. Rewoldt, D. Roberts, J. Rogers, A. L. Roquemore, E. Ruskov, S. A. Sabbagh, M. Sasao, G. Schilling, J. Schivell, G. L. Schmidt, S. D. Scott, I. Semenov, S. Sesnic, C. H. Skinner, D. Spong, B. C. Stratton, J. D. Strachan, W. Stoidiek, E. Synakowski, H. Takahashi, W. Tang, G. Taylor, J. Terry, W. Tighe, J. R. Timberlake, A. von Halle, S. von Goeler, R. White, J. R. Wilson, K. L. Wong, G. A. Wurden, K. M. Young, M. C. Zarnstorff and S. J. Zweben, *Plasma Phys. Controlled Fusion* **37 Suppl. 11A**, A69 (1995).
- <sup>5</sup>The JET Team (presented by M. Keilhacker), *Plasma Phys. Controlled Fusion* **37 Suppl. 11A**, A3 (1995).
- <sup>6</sup>D. Johnson, D. Dimock, B. Grek, D. Long, D. McNeill, R. Palladino, J. Robinson and E. Tolnas, *Rev. Sci. Instrum.* **56**, 1015 (1985).
- <sup>7</sup>D. Johnson, N. Bretz, D. Dimock, B. Grek, D. Long, R. Palladino and E. Tolnas, *Rev. Sci. Instrum.* **57**, 1856 (1986).
- <sup>8</sup>B. W. Brown, C. Gowers and P. Neilsen, JET-TN (91) 03, "Lidar Window Transmission Monitors on JET" (1991).
- <sup>9</sup>K. Okazaki, H. Oyama, Y. Ishibe, S. Kato, Y. Sakamoto, S. Ameyama, T. Matsuda, Y. Tsurita, Y. Hori, K. Akaishi, K. Kawahata and N. Noda, *J. Nucl. Mater.* **145-147**, 761 (1987).

- <sup>10</sup>K. Narihara and S. Hirokura, *Rev. Sci. Instrum.* **63**, 3527 (1992).
- <sup>11</sup>B. W. Brown, C. Gowers, P. Neilsen, and B. Shunke, *Rev. Sci. Instrum.* **66**, 3077 (1995).
- <sup>12</sup>C. W. Gowers, B. W. Brown, H. Fajemirokun, P. Nielsen, Y. Nizienko and B. Schunke, *Rev. Sci. Instrum.* **66**, 471 (1995).
- <sup>13</sup>H. Yoshida, K. Shimizu, H. Shirai, K. Tobita, Y. Kusama, H. Kubo, Y. Koide, A. Sakasai, T. Fukuda, K. Nagashima, O. Naito, S. Tsuji, N. Hosogane and JT-60 Team, in *Proceedings of 15th European Conference on Controlled Fusion and Plasma Heating* (European Physical Society, Dubrovnik, May 16-20, 1988 ), Part I, p. 163.
- <sup>14</sup>G. K. Bhagavat and K. D. Nayak, in *Proceedings of 7th Int. Vac. Congr. and 3rd Int. Conf on Solid Surfaces* (Vienna, 1977 ), Vol. 2, p. 1879.
- <sup>15</sup>S. Murahashi, M. Imoto and H. Tani, *Synthetic Macromolecule IV* (Asakura Publishing Company Ltd., Tokyo, Japan, 1975).
- <sup>16</sup>S. Y. Kim and E. A. Irene, *Rev. Sci. Instrum.* **66**, 5277 (1995).
- <sup>17</sup>H. Yoshida, O. Naito, O. Yamashita, S. Kitamura, A. Nagashima and T. Matoba, *Rev. Sci. Instrum.* **66**, 143 (1995).

Table I

Experimental periods and operational records for the coated windows illustrated in Fig. 2: (a) for windows at *IN1A* port during 1987 to 1989, (b) for windows at *IN1A* port during 1991 to 1995 and (c) for windows at *R1* port during 1991 to 1995

(a)

Window Sample No.	Window Location	Experimental Period	Plasma Configuration	Number of Plasma Shots	Exposure Time to TDC	Number of Disruptions	The First Wall Material	Divertor Area Material
1	IN1A	Jun.-Oct. '87	Outer X-Point & Limiter	1611	4.0 hr	458	TiC coated Mo	TiC coated Mo
2	↑	Jun.-Oct. '88	Lower X-Point & Limiter	1787	5.4 hr	506	Graphite & TiC coated Mo	Graphite
3	↑	Jan.-Apr. '89	↑	1351	35.7 hr	324	↑	↑
4	↑	Jun.-Oct. '89	↑	1905	20.0 hr	482	↑	↑

(b)

Window Sample No.	Window Location	Experimental Period	Plasma Configuration	Number of Plasma Shots	Exposure Time to TDC/GDC	Boronization with GDC	The First Wall Material	Divertor Area Material
5	IN1A	Jun.-Oct. '91	Lower X-Point	1086	None	—	Graphite	CFC
6	↑	Jan.-Oct. '92	↑	1880	None	Yes	↑	↑
7	↑	Jan.-Oct. '93	↑	2335	None	Yes	↑	CFC partially with B <sub>4</sub> C conversion
8	↑	Jan.-Oct. '94	↑	2776	None	Yes	↑	↑
9	↑	Jan.-Apr. '95	↑	928	None but stained by foreign matters	Yes	↑	↑
10	↑	Jun.-Oct. '95	↑	1580	None	Yes	↑	↑

(c)

Window Sample No.	Window Location	Experimental Period	Plasma Configuration	Number of Plasma Shots	Exposure Time to TDC/GDC	Boronization with GDC	The First Wall Material	Divertor Area Material
11	R1	Jun.-Oct. '91	Lower X-Point	1086	None	—	Graphite	CFC
12	↑	Jan.-Jun. '92	↑	1017	several hours (Shutter Trouble)	Yes	↑	↑
13	↑	Jul.-Oct. '92	↑	863	None	Yes	↑	↑
14	↑	Jan.-Jun. '93	↑	1334	a few hours	Yes	↑	CFC partially with B <sub>4</sub> C conversion
15	↑	Jul.-Oct. '93	↑	1001	None	Yes	↑	↑
16	↑	Jan.-Oct. '94	↑	2776	None	Yes	↑	↑
17	↑	Jan.-Oct. '95	↑	2568	None	Yes	↑	↑



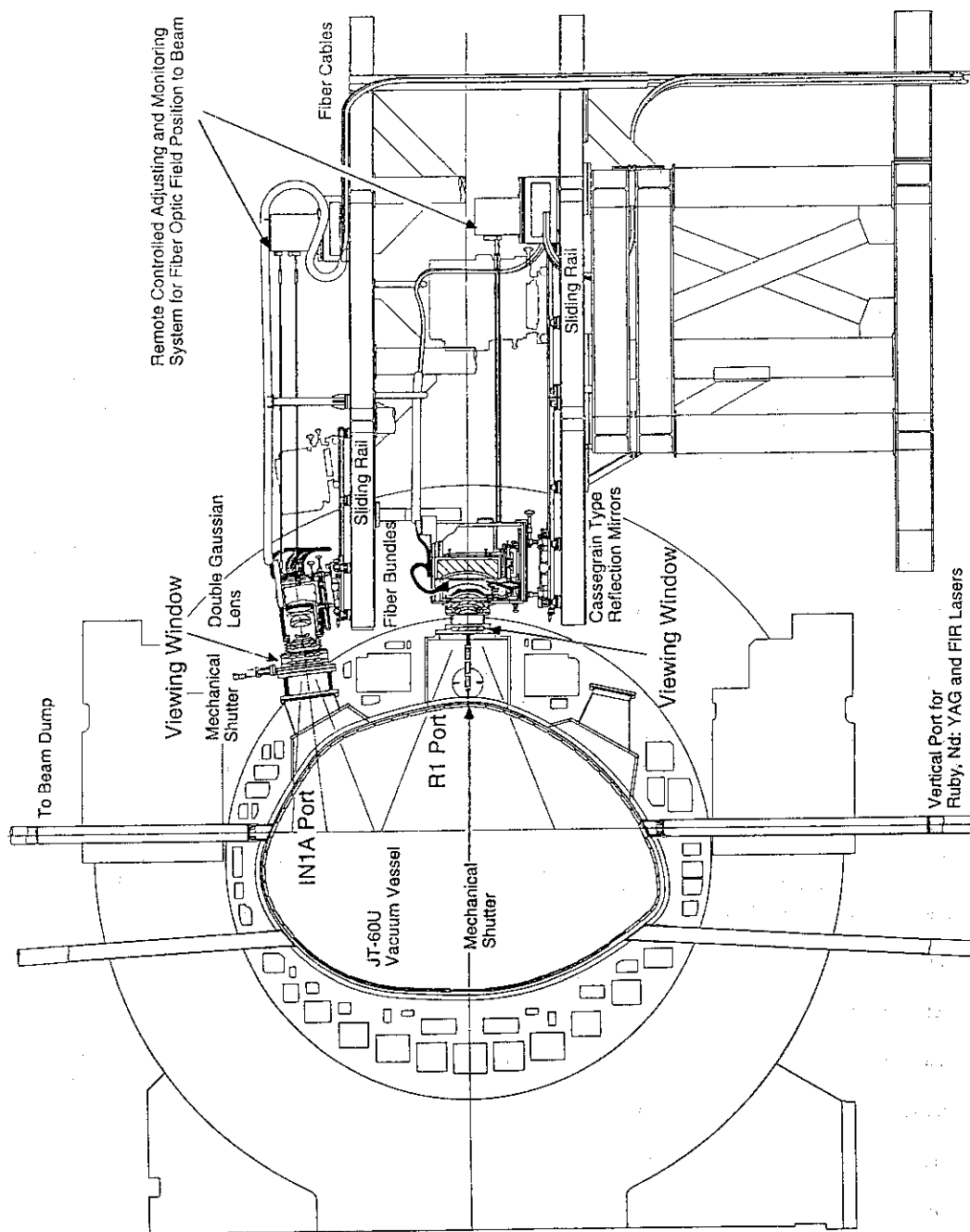


Figure 1

Schematic layout for the JT-60U Thomson scattering system, where the two viewing windows at *IN1A* port and *R1* port, and the corresponding collection optics with remote-controlled mechanical shutters are shown

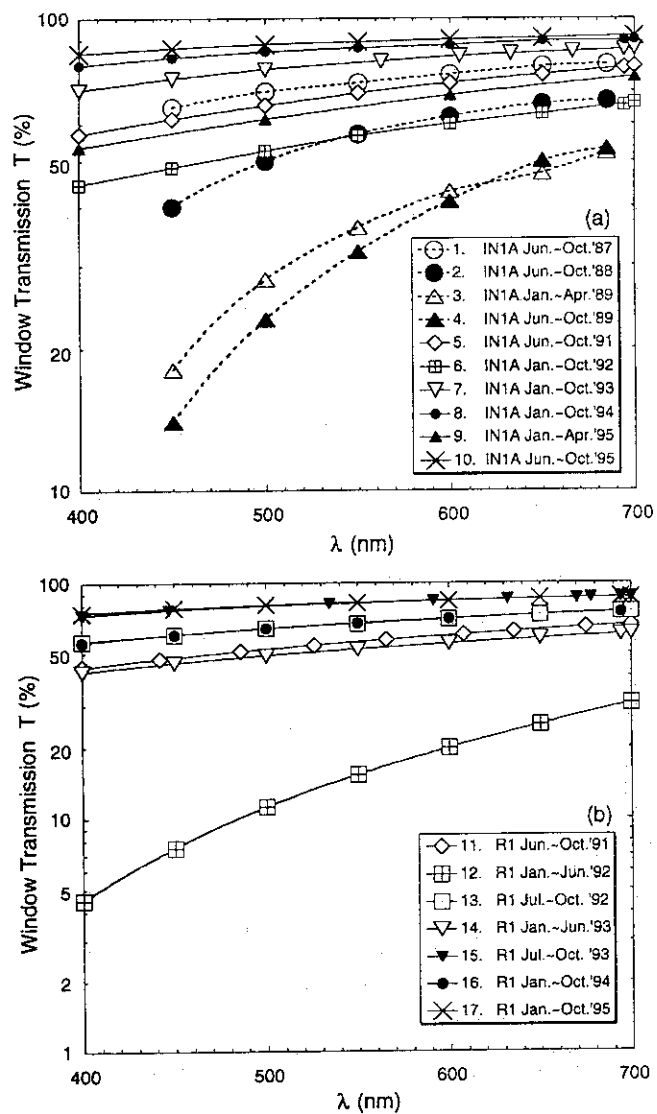


Figure 2

Transmissions of the viewing windows in the JT-60U Thomson scattering system for (a) *INIA* port and (b) *R1* port measured just after each experimental campaign. The number on the right side of each symbol means the sample number of the coated window that is listed with the experimental period in TABLE I

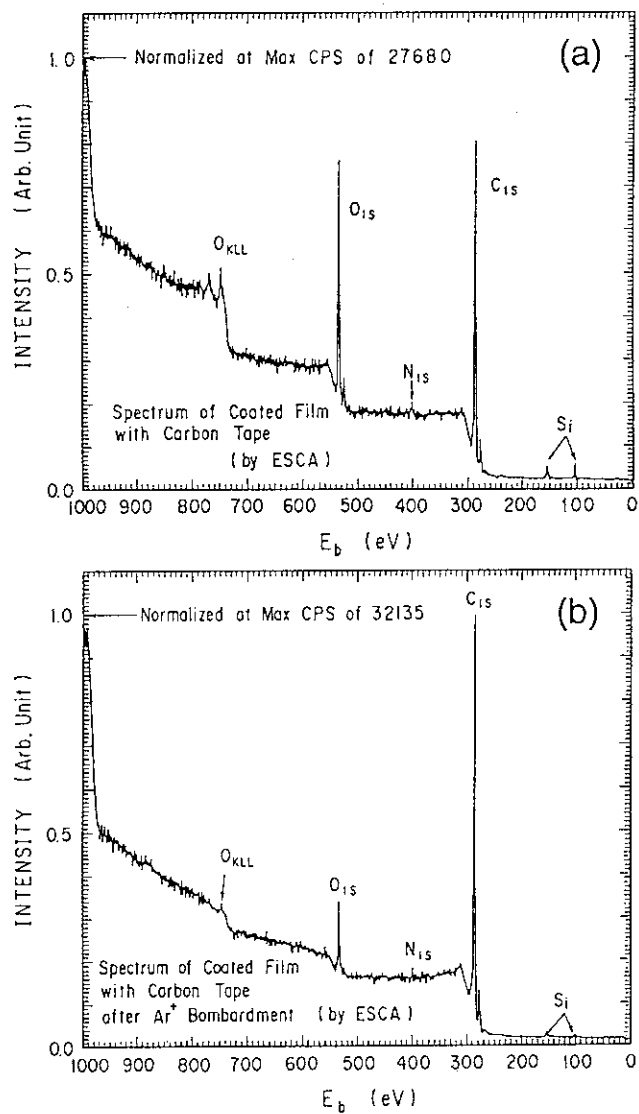


Figure 3

Wide scanning ESCA spectrum of deposited film (a) with carbon tape and (b) after Ar<sup>+</sup> bombardment

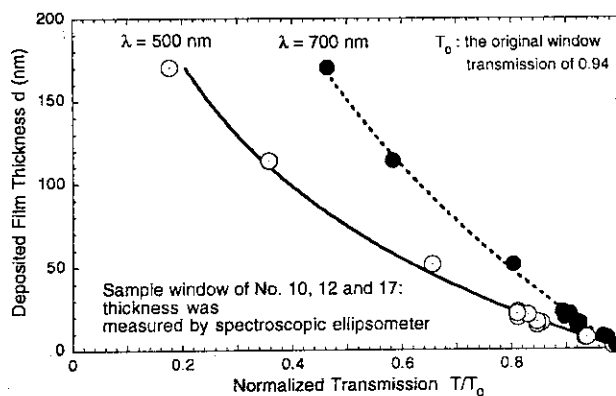


Figure 4

Deposited film thickness  $d$  measured by a spectroscopic ellipsometer is plotted against a fractional window transmission  $T/T_0$  at the wavelength of 500 and 700 nm, where  $T_0$  is the original window transmission of 94%

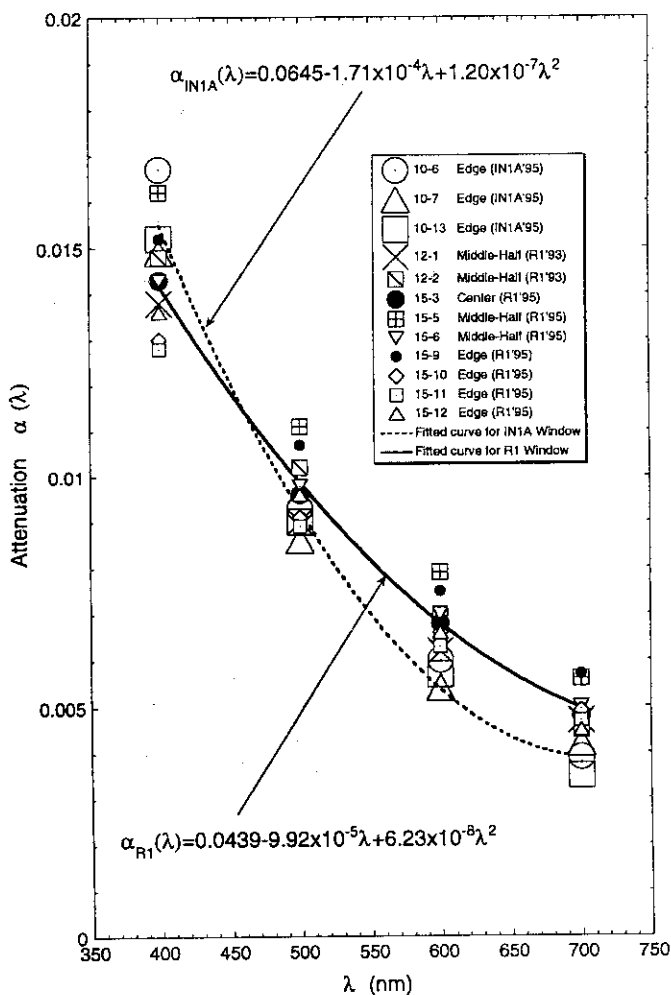


Figure 5

Estimated attenuation of deposited film  $\alpha(\lambda)$  plotted against wavelength, using the same data set as in Fig. 4. The regression curves of attenuation are obtained separately for the deposited films of *INIA* port and *R1* port

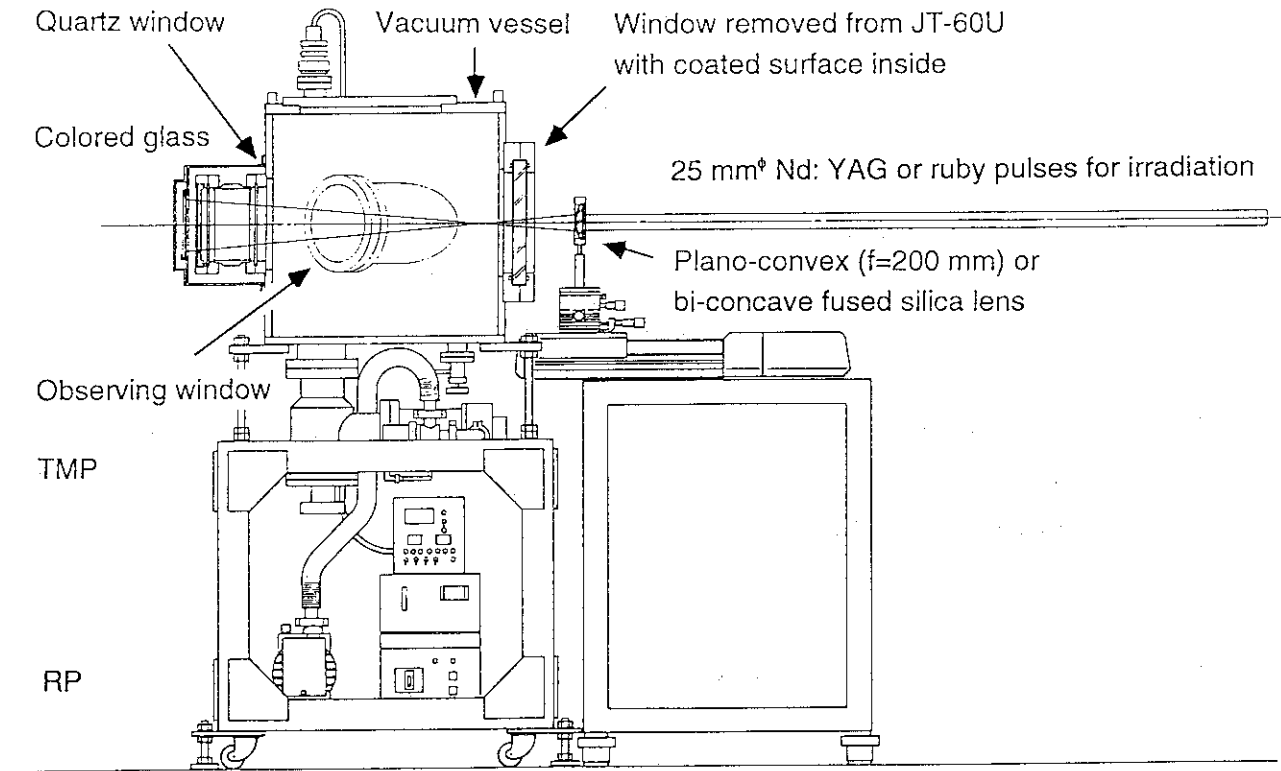


Figure 6  
Testing arrangement for laser-blow-off-based window cleaning

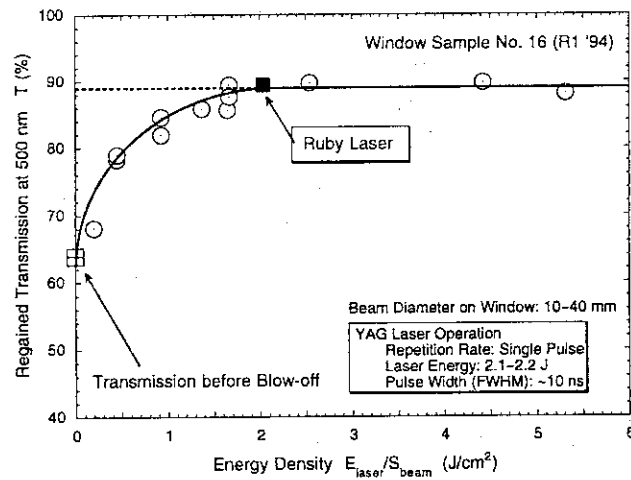


Figure 7  
Window transmission after the blow-off cleaning plotted against laser energy density per pulse

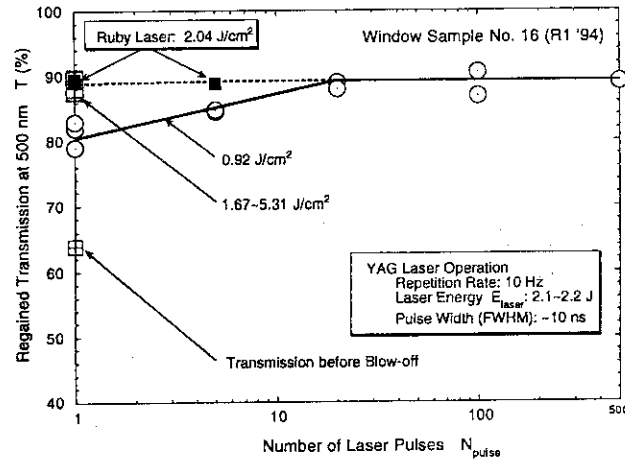


Figure 8  
Window transmission after the blow-off cleaning plotted against number of laser pulses

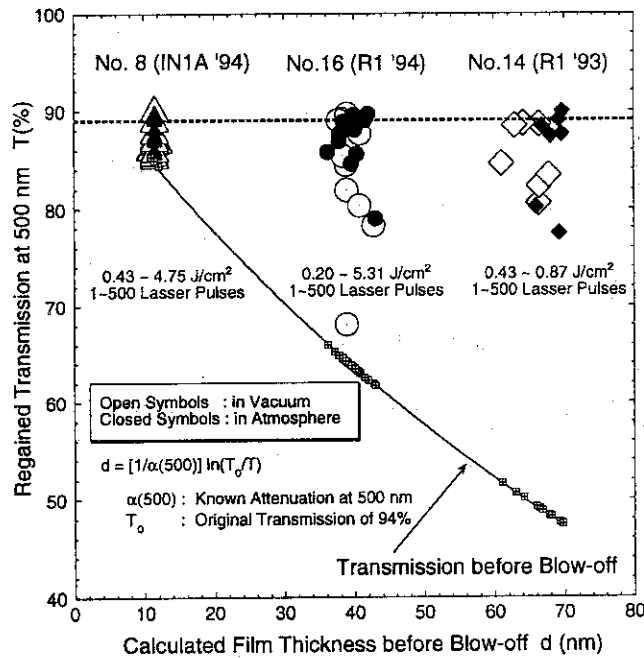


Figure 9  
Window transmission at 500 nm before and after the blow-off cleaning plotted against film thickness. Three windows with different film thickness were irradiated by the Nd: YAG laser with indicated energy density and number of pulses under the condition *in atmosphere* and *in vacuum*. The film thickness was calculated using the known attenuation given in Eq. (3) or (4) and the corresponding transmission

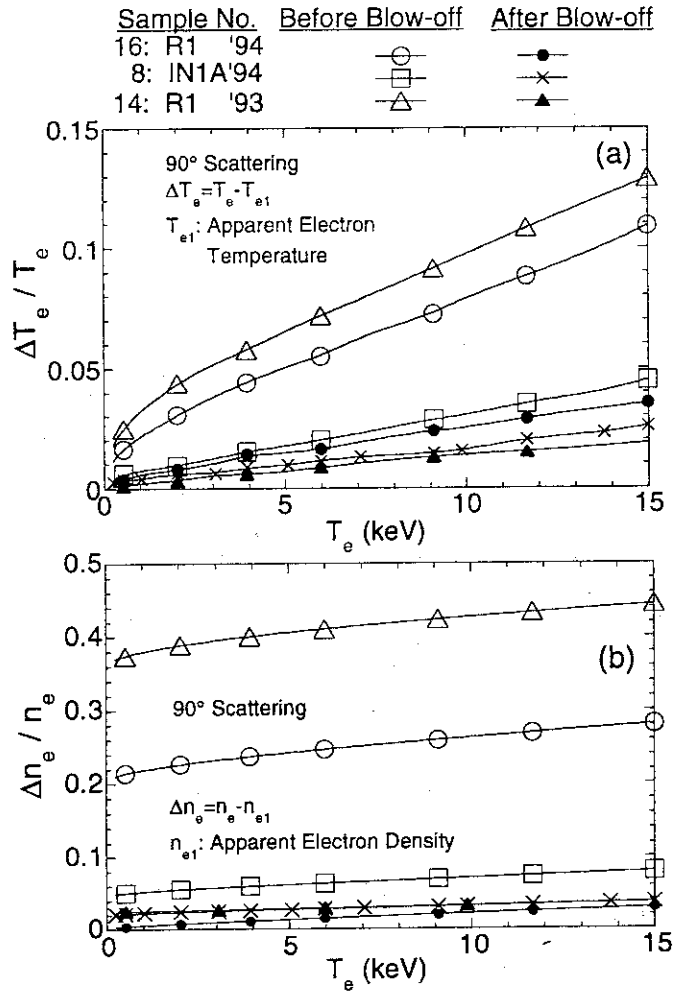


Figure 10

Systematic errors of (a)  $T_e$  and (b)  $n_e$  measurement before and after the blow-off cleaning plotted as a function of electron temperature

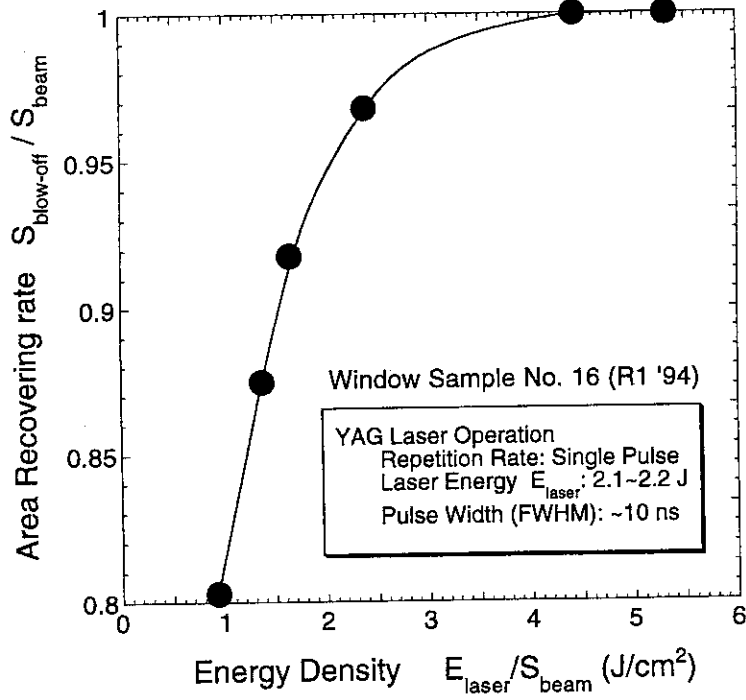


Figure 11

Area recovering rate  $\eta$  plotted against laser energy density per pulse

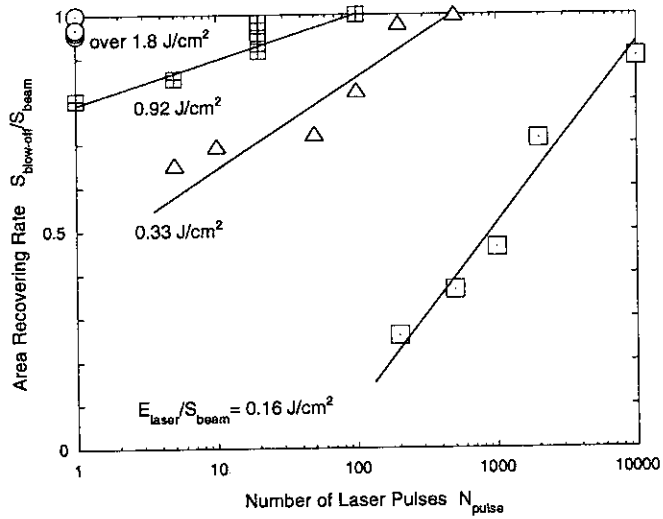


Figure 12

Area recovering rate  $\eta$  plotted against the number of laser pulses with the energy density of 0.16 J/cm<sup>2</sup> (window sample No. 9), 0.33 J/cm<sup>2</sup> (No. 12), 0.92 J/cm<sup>2</sup> and over 1.8 J/cm<sup>2</sup> (No. 16). For the blow-off operation with 0.16 J/cm<sup>2</sup>, the transmission recovering rate did not exceed about 0.9 within up to 10<sup>4</sup> successive laser pulses



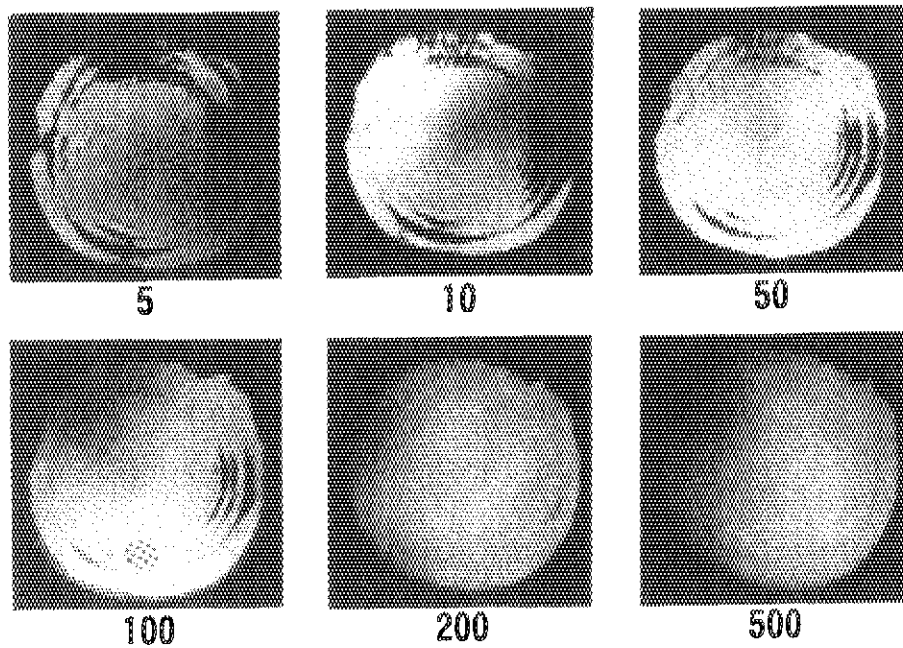


Figure 13

A series of photographs which shows the extension of the blown-off area with increase in the irradiation number of successive Nd: YAG laser pulses. These photographs are identical with the plotted data of  $\epsilon = 0.33 \text{ J/cm}^2$  in Fig. 11. The beam diameter is about 30 mm on the film surface of the sample window No. 12. The figure indicated below each photograph is the irradiation number

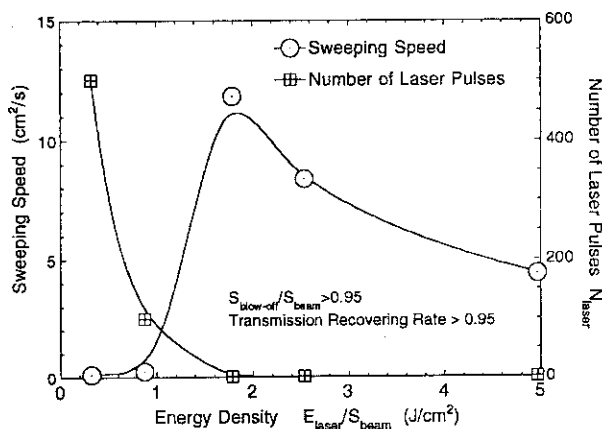


Figure 14

Sweeping speed  $S_p$  and the number of successive laser pulses needed for the indicated conditions plotted as a function of  $\epsilon$

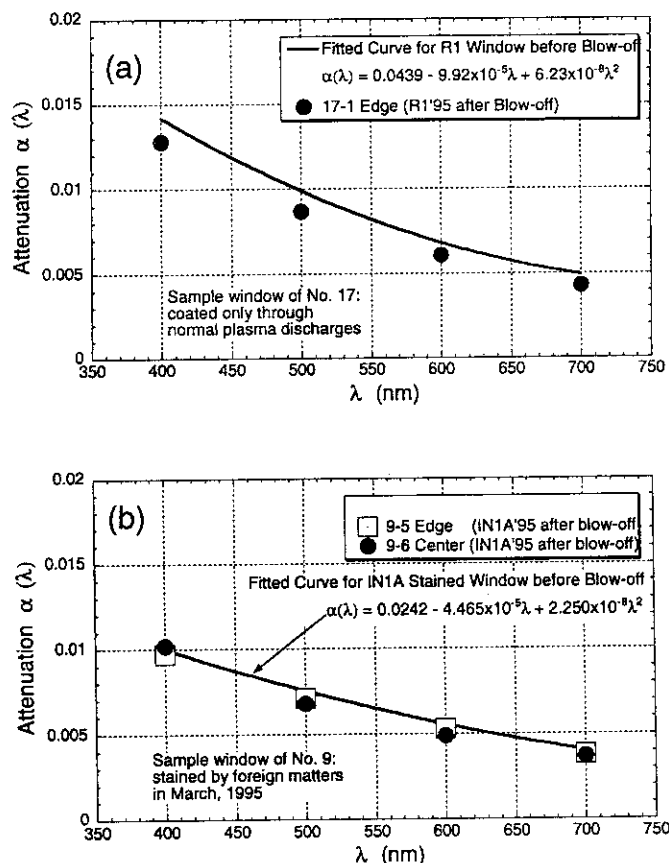


Figure 15

Comparison of the attenuation before and after the blow-off cleaning for (a) the *RI* window of sample No. 17, and (b) the *INIA* of sample No. 9 window not only slightly coated through normal discharges but strongly stained by foreign matters